Bulletin of the Seismological Society of America, Vol. 107, No. 5, pp. 2055–2066, October 2017, doi: 10.1785/0120160252

A Study of Vertical-to-Horizontal Ratio of Earthquake Components in the Gulf Coast Region

by Alireza Haji-Soltani, Shahram Pezeshk, Mojtaba Malekmohammadi, and Arash Zandieh

Abstract A new ground-motion prediction model is developed for the response spectral ratio of vertical-to-horizontal (V/H) components of earthquakes for the Gulf Coast region. The proposed V/H response spectral ratio model has the advantage of considering the earthquake magnitude, source-to-site distance, and the shear-wave velocity of soil deposits in the upper 30 m of the site (V_{S30}) for the peak ground acceleration, and a wide range of spectral periods (0.01–10.0 s). The model is based on a comprehensive set of regression analyses of the newly compiled Next Generation Attenuation-East database of available central and eastern North America recordings with the moment magnitudes $\mathbf{M} \geq 3.4$ and the rupture distances $R_{\mathrm{Rup}} < 1000$ km. The 50th percentile (or median) pseudospectral acceleration values computed from the orthogonal horizontal components of ground motions rotated through all possible nonredundant rotation angles, known as the RotD50 (Boore, 2010), is used along with the vertical component to perform regression using a nonlinear mixed-effects regression algorithm. The predicted V/H ratios from the proposed model are compared with the recently published V/H spectral ratio models for different regions. The derived V/H ratios can be used to develop the vertical response spectra for the sites located within the Gulf Coast region, which include the Mississippi embayment.

Introduction

Seismic design of structures is fundamentally governed by the horizontal component of ground motion, and the effects of the vertical component of earthquakes have long been neglected in structural design. However, destructive earthquakes such as the Northridge, California (1994), Kobe, Japan (1995), and Chi-Chi, Taiwan (1999) have provided an emerging body of evidence that the vertical component of earthquakes is more important than previously thought. These new levels of information reveal the destructive potential of the vertical component of earthquakes and suggest that the effects of both vertical and horizontal components of ground motions should be considered in the seismic design of structures. The effects of the vertical component of earthquakes on structural systems have been addressed in different studies (Saadeghvaziri and Foutch, 1991; Papazoglou and Elnashai, 1996; Yu *et al.*, 1997; Bozorgnia and Campbell, 2004a; Kunnath *et al.*, 2008).

There are basically two main approaches in developing a vertical design response spectrum for a study site. The first is to perform a probabilistic seismic-hazard analysis (PSHA) using vertical ground-motion prediction equations (GMPEs) to estimate the vertical ground-motion hazard. For instance, western United States (WUS) vertical GMPEs are developed using the Pacific Earthquake Engineering Research Center–Next Generation Attenuation (PEER NGA)-West2 ground-motion database for the vertical component of peak ground acceleration (PGA), peak ground velocity (PGV), and pseudospectral acceleration (PSA) values by Chiou and Youngs (2013) in PEER (2013), Bozorgnia and Campbell (2016a), Stewart *et al.* (2016), and Gülerce *et al.* (2017). However, there are some drawbacks to applying this approach in other regions. First, there is lack of region-specific vertical GMPEs in areas such as central and eastern North America (CENA) due to data limitations. Second, there is a possible mismatch between the vertical and the horizontal controlling earthquakes resulting from the deaggregation of hazard in terms of vertical and horizontal response spectral ordinates.

The second approach is to use the vertical-to-horizontal (V/H) spectral ratio of the ground motion to adjust an available horizontal design spectrum to a vertical spectrum. In this case, PSHA is performed using the horizontal GMPEs, and the resulting horizontal design spectrum will be scaled to the vertical orientation. This would solve the aforementioned problem associated with the first approach by preserving the same earthquake scenario resulting from the deaggregation. The V/H spectral ratios are usually expressed as a function of earthquake magnitude, source-to-site distance, and site classification. The V/H spectral ratios of ground motions have been obtained in two ways. In the first method, the V/H spectral ratio model is estimated as the ratio of the vertical GMPEs and the horizontal one for a given scenario (Ambraseys and Douglas, 2003; Bozorgnia and Campbell, 2004b, 2016b; Sedaghati and Pezeshk, 2017). The second method is based on the regression analyses on the V/H spectral ratios obtained from empirical data (Bommer *et al.*, 2011; Gülerce and Abrahamson, 2011; Akkar *et al.*, 2014).

A list of recent studies on the relationship between the vertical and horizontal components of earthquake ground motion is provided in Bozorgnia and Campbell (2016b). For example, Siddiqqi and Atkinson (2002) used the ratio of the horizontal-to-vertical (H/V) components of ground motion to determine the frequency-dependent amplification inherent in hard-rock sites across Canada. They used a Fourier spectra database compiled from 424 earthquakes of magnitude greater than or equal to 2, recorded on 32 three-component stations of the Canadian National Seismograph Network, all sited on rock. Their results showed that the H/V ratio for rock sites is poorly frequency dependent and does not vary considerably across Canada. The H/V ratios were increasing from a factor near unity at 0.5 Hz to a maximum in the range from 1.2 to 1.6 at 10 Hz.

Zandieh and Pezeshk (2011) studied the Fourier domain H/V spectral ratios in the New Madrid Seismic Zone to capture the amplification effect of local soil sediments on earthquake ground motion. They used 500 broadband seismograms from 63 events of moment magnitude **M** 2.5–5.2, recorded on broadband stations in the Mississippi embayment. They compared the H/V spectral ratios with the theoretical quarter-wavelength approximation and showed that the H/V spectral ratios could be a first estimate of the site amplifications.

Seismic codes suggested a variety of V/H models to obtain the vertical design spectrum. Regulatory Guide 1.60 (1973) is among the first seismic codes that considered obtaining the vertical design spectrum from the horizontal spectrum using the V/H spectral ratio model. McGuire *et al.* (2001) studied the V/H spectral ratios for rock site conditions in WUS and central and eastern United States (CEUS) to update Regulatory Guide 1.60 values for the V/H spectral ratios. Their V/H spectral ratios were presented for a range of expected horizontal PGA values to accommodate the magnitude and distance dependency. For very hard-rock conditions in CEUS, very few recordings were available for earthquakes with magnitudes $\mathbf{M} > 5$. Furthermore, McGuire *et al.* (2001) studied recordings of the Saguenay event and the only three available recordings of the Nahanni and Gazli earthquakes. They observed that the very few data in CEUS pointed to the fact that the V/H spectral ratios might be high at very close rupture distances to the CEUS earthquakes. They indicated that data from more distant events have lower V/H spectral ratios for the WUS rock sites than the CEUS rock sites. To develop recommended V/H spectral ratios for applications in CEUS, they used a modified point-source model to predict the general trend in V/H spectral ratios at rock sites from the 1989 magnitude 6.9 Loma Prieta earthquake in WUS. The point-source model predicted a peak in the V/H spectral ratios near 60 Hz corresponding to the peak in WUS ratios but moved from about 15 to 20 Hz to ~60 Hz. The V/H spectral ratios in the CEUS model showed higher values at low frequencies for less than 3 Hz, as compared to the WUS ratios, consistent with available data. McGuire *et al.* (2001) recommended that V/H spectral ratios for rock sites in CEUS can be developed by shifting the WUS ratios to match the peaks corresponding to about 60 Hz. The WUS levels at low frequency were also increased by ~50%. National Earthquake Hazards Reduction Program (NEHRP, 2009) recommends a vertical design spectrum, which is based on site class, SDS (design earthquake spectral response acceleration parameter at short period), and SS (the mapped maximum credible earthquake spectral response parameter at short period). The vertical design spectrum suggested by NEHRP (2009) is mainly based on the study by Bozorgnia and Campbell (2004b).

Gülerce and Abrahamson (2011) developed GMPEs to predict the V/H ratios of response spectra. They reviewed methods for constructing the site-specific vertical design spectra from a Uniform Hazard Spectrum and a conditional mean spectrum to be consistent with PSHA. The functional form for their V/H spectral ratios is consistent with the horizontal GMPEs developed by Abrahamson and Silva (2008). They used the PEER NGA-West1 Project database, which consists of 2684 sets of recordings from 127 earthquakes. Their functional form to predict the V/H ratio is dependent on earthquake magnitude, source-to-site distance, and type of faulting. They also included the functional form developed by Walling *et al.* (2008) to predict the effects of the nonlinear soil behavior in their V/H ratio model. Bommer *et al.* (2011) reviewed V/H ratio models by different seismic codes and regulations, such as the Regulatory Guide 1.60, McGuire *et al.* (2001), the Eurocode 8 (2004), and the NEHRP (2009). Their proposed model is based on 1296 accelerograms from 392 events occurring in Europe, the Middle East, and surrounding regions and predicts V/H spectral ratios for PGA and spectral accelerations from 0.02 to 3.0 s. Although their model predicts lower values for the V/H spectral ratio, it is in general agreement with the model developed by Gülerce and Abrahamson (2011), which is based on the data from western North America. Their model can be used for a magnitude range of 4.5–7.6 and distances up to 100 km.

Akkar *et al.* (2014) developed a V/H spectral ratio model for shallow active crustal regions in Europe and the Middle East. Their model is a function of magnitude, source-to-site distance, and style of faulting and includes a site response term that uses a continuous function of V_{S30} to capture soil nonlinearity. Their proposed V/H ratio model is compatible with the horizontal GMPEs of Akkar *et al.* (2013a,b). They showed that for larger magnitudes, their model predicts larger V/H spectral ratios toward lower frequencies compared to the Bommer *et al.* (2011) model. For small magnitudes, the Bommer *et al.* (2011) model gives larger V/H estimates. They suggested that the different functional forms

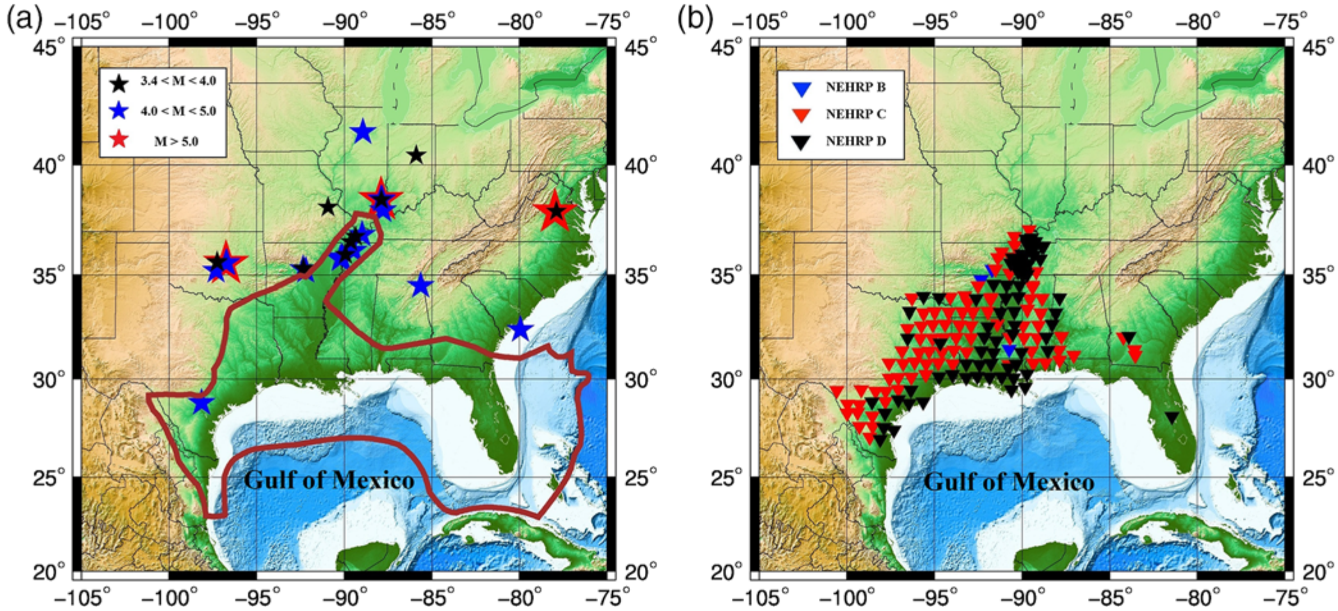

Figure 1. (a) Location of earthquakes and the Gulf Coast region. (b) Recording stations within the Gulf Coast region in terms of National Earthquake Hazards Reduction Program (NEHRP) site classification. The color version of this figure is available only in the electronic edition.

as well as the resolution of the database could cause these discrepancies. Sedaghati and Pezeshk (2017) developed horizontal and vertical GMPEs using active crustal earthquakes occurring within the Iranian plateau. Their database includes 688 records from 152 earthquakes of $4.7 \le \mathbf{M} \le 7.4$ and Joyner–Boore distances up to 250 km. They also calculated the V/H response spectral ratios and showed that the median V/H ratios increase with decreasing distance. Bozorgnia and Campbell (2016b) developed a ground-motion model (GMM) for the V/H ratios of PGA, PSA, and PGV. Their V/H spectral ratio model is based on their horizontal and vertical GMMs (Campbell and Bozorgnia, 2014; Bozorgnia and Campbell, 2016a), which were developed as part of the NGA-West2 research program (Bozorgnia *et al.*, 2014). They showed that their V/H model predictive power is not significantly influenced by excluding deep basin effects and soil nonlinearity from the vertical GMM.

In the present study, we use the first approach to propose a new model for the median V/H response spectral ratio for the Gulf Coast region. The Gulf Coast region is centrally located between the Appalachian Mountains and the eastern Rocky Mountains and includes the Mississippi embayment as shown in Figure 1. It has been shown that earthquake recordings in the Gulf Coast region exhibit significantly different ground-motion attenuation compared to the rest of CEUS because of the thick sediments in the region (Dreiling *et al.*, 2014). Therefore, the V/H response spectral ratio model is developed based on a subset of the NGA-East database (Goulet *et al.*, 2014) specific to the Gulf Coast region. The proposed model can be used to scale the available horizontal CENA GMPEs, such as Darragh *et al.* (2015), Frankel (2015), Graizer (2015), Hassani *et al.* (2015), Shahjouei and Pezeshk (2015), and Yenier and Atkinson (2015) in PEER (2015a), and Pezeshk *et al.* (2015). It should be mentioned that the aforementioned GMPEs are adjusted for the Gulf Coast region in PEER (2015b).

Strong-Motion Database and Record Processing

We used a subset of the NGA-East database in which only the ground motions that are recorded within the Gulf Coast region with $\mathbf{M} \ge 3.4$ are selected (Fig. 1). The Gulf Coast region boundaries are defined based on the NGA-East regionalization (Dreiling *et al.*, 2014). As can been seen from Figure 1, there are a limited number of events within the Gulf Coast region. Therefore, we expanded our rupture distance to 1000 km, which adds the events beyond the Gulf Coast region to our database. We only considered the records with significant travel path located within the Gulf region. NEHRP site class E (soft-soil) sites are excluded from consideration because of their complex site-response characteristics and their potential for nonlinear site effects. We also included time histories from the 2011 **M** 5.68 Sparks, Oklahoma, event and its aftershocks because it was one of the relatively large-magnitude earthquakes that happened close to the study area. Figure 2 displays the magnitude–distance distribution of the selected 978 recordings in terms of style of faulting and the NEHRP site classification: rock ($760 \le V_{S30} \le 1500$ m/s), soft rock ($360 \le V_{S30} > 760$ m/s), and stiff soil ($180 \le V_{S30} > 360$ m/s).

The V/H models are needed to be developed for a broad range of frequencies to satisfy the structural analysis requirements. The vertical component of ground motion is rich in higher frequencies. Therefore, V/H ratios are primarily a

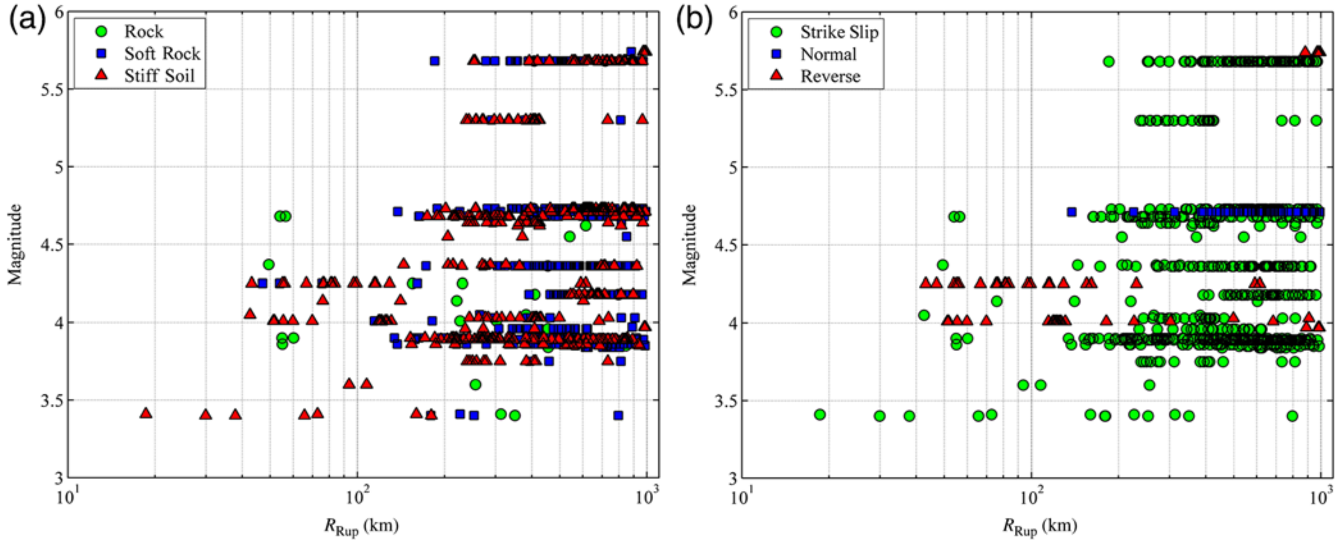

Figure 2. Magnitude versus distance distribution of the considered records in terms of (a) NEHRP site classification and (b) style of faulting. The color version of this figure is available only in the electronic edition.

high-frequency phenomenon. However, strong ground motion records may contain high-frequency noise, which needs to be removed before computing PSA values. The accuracy of PSA values at high frequencies obtained from the filtered strong ground motions has been investigated in different studies (e.g., Boore and Bommer, 2005; Akkar and Bommer, 2006; Akkar *et al.*, 2011; Douglas and Boore, 2011; Graizer, 2012; Boore and Goulet, 2014). Douglas and Boore (2011) showed that in the tectonically active regions with high attenuation, such as WUS, the high-frequency content of the strong ground motions are naturally removed. Ground motions at frequencies much lower than the oscillator frequency would control the response of a high-frequency oscillator, and PSA values would not be affected significantly by the low-pass filters in data processing. However, this might not be the case for the regions with comparable lower anelastic attenuation, such as CENA, where the ground motions are recorded on very hard-rock sites with a significant amount of energy at high frequencies. Akkar *et al.* (2011) studied the usable high-frequency range of the European strong-motion database to find reliable criteria for identifying the degree to which PSA values at the high frequencies will be changed by the low-pass filtering. They concluded that the effect of low-pass filtering on the PSA values becomes negligible for corner frequencies lower than 20 Hz. For the NGA-East database, the low-pass and high-pass corner frequencies are multiplied by a factor of 0.8 and 1.25, respectively, to calculate the minimum and maximum usable frequencies for each filtered record. The corner frequencies are selected on an individual basis for filtering the vertical and horizontal components (Goulet *et al.*, 2014).

In this study, for the lowest usable frequency, we considered the maximum of the minimum usable frequencies of the horizontal and vertical components in our regression analysis. Not all of the selected time series from the NGA-East database are low-pass filtered. For those low-pass filtered records, we followed the Douglas and Boore (2011) procedure to determine how the PSAs are affected by the low-pass filtering. Douglas and Boore (2011) used the ratio between the peak of the Fourier amplitude spectrum (FAS) of the acceleration and the level of high-frequency noise, called RFAS, and showed that if RFAS is less than 10, the PSA values will be affected insignificantly (less than 15% difference) by low-pass filtering. Consequently, 18 records with RFAS values less than 10 are not considered in our regression analysis. Akkar *et al.* (2011) showed that, while RFAS could be used as an *a priori* useful tool to find the records for which the high-frequency portion of the response spectral ordinates has been highly influenced by filtering, it would also be useful to investigate how the oscillator response interacts with the frequency content of the ground motion using basic structural dynamics. Consequently, we followed the Akkar *et al.* (2011) procedure to make sure that we used only reliable records in our regression analysis. A total number of 17 records with RFAS $\geq$ 10 were found, for which the PSA values for frequencies greater than 50 Hz were significantly affected by the low-pass filtering. These recordings were also removed, and the remaining 943 recordings were used in our regression analysis. Major features of the selected earthquakes are summarized in Table 1. It should be noted that there are no events with $\mathbf{M} > 5.74$ in the study. Because the result of the proposed model has not been verified with actual recordings of $\mathbf{M} > 5.74$ for the study region, results from this study should be used with extra caution for such events.

Functional Form and Regression Analysis

The PSAs from the NGA-East database are the 50th percentile (or median) PSA value calculated from the orthogonal

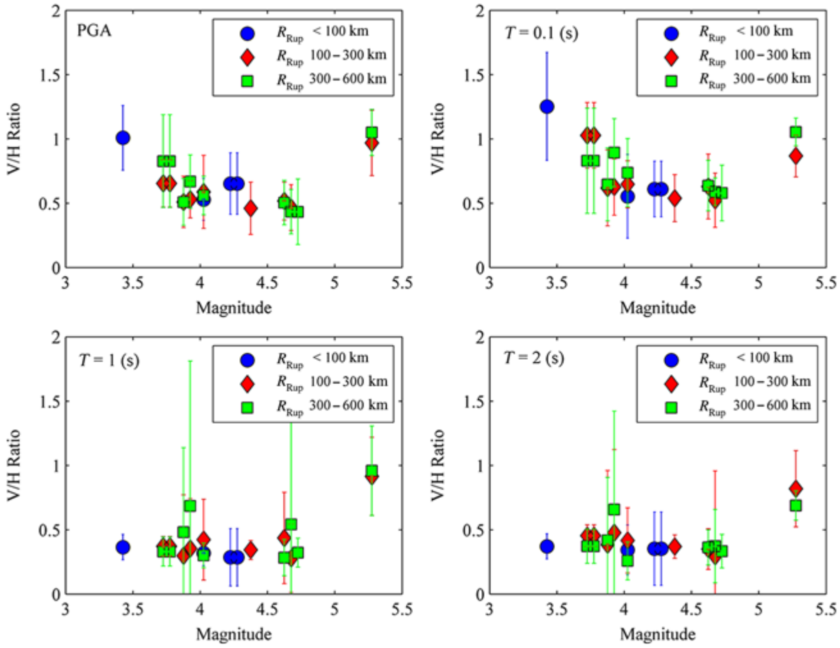

Figure 3. Median vertical-to-horizontal (V/H) response spectral ratios as a function of magnitude for soil sites ($V_{S30} = 270$ m/s). Error bars represent the one standard deviation of each magnitude bin. The color version of this figure is available only in the electronic edition.

horizontal ground motions rotated through all possible nonredundant rotation angles, known as the RotD50 (Boore, 2010). The RotD50 values are used along with the vertical PSA values to perform a parametric regression analysis in which coefficients are calibrated using the nonlinear mixed-effects algorithm (Lindstrom and Bates, 1990) using the MATLAB functions of *nlmefit* and *fitlmematrix* (MathWorks Inc., 2015). The general functional form to be considered in the regression analysis is a function of source, path, and site terms as

$$\ln(\mathrm{V/H}) = f_{\mathrm{source}} + f_{\mathrm{path}} + f_{\mathrm{site}} + \Delta_{es}, \quad (1)$$

in which f_{source} is the source term, f_{path} is the path term, f_{site} is the site term, and Δ_{es} is a random variable describing the total variability of the earthquake ground motion. To select the most appropriate functional form to perform the regression analysis, we investigated the trend of the median V/H response spectral ratios as a function of estimator parameters for each term of equation (1). We investigated various trial functional forms to find the most appropriate one by comparing the predicted models with our database and using statistical tools such as the Akaike information criteria (AIC) and Bayesian information criteria (BIC) values and the logarithm of their likelihoods. The AIC and BIC measure the quality of the considered statistical models relative to the other models for a given database (Burnham and Anderson, 2002).

Table 1
Earthquakes Used in this Study

Event Name	Date (yyyy/mm/dd)	**M**	Latitude (°)	Longitude (°)	Number of Records
Comal	2011/10/20	4.71	28.81	−98.15	56
Charleston	2002/11/11	4.03	32.40	−79.94	4
FtPayne	2003/04/29	4.62	34.49	−85.63	4
Slaughterville	2010/10/13	4.36	35.20	−97.31	49
Enola	2001/05/04	4.37	35.21	−92.19	7
Greenbrier	2011/02/28	4.68	35.27	−92.34	88
Guy	2010/10/15	3.86	35.28	−92.32	51
Guy	2010/11/20	3.90	35.32	−92.32	60
Sparks	2011/11/06	5.68	35.54	−96.75	136
Lincoln	2010/02/27	4.18	35.55	−96.75	42
Sparks	2011/11/05	4.73	35.57	−96.70	133
Jones	2010/01/15	3.84	35.59	−97.26	10
Arcadia	2010/11/24	3.96	35.63	−97.25	27
MilliganRdg	2005/02/10	4.14	35.75	−90.23	6
ShadyGrove	2005/05/01	4.25	35.83	−90.15	27
Blytheville	2003/04/30	3.60	35.94	−89.92	4
Miston	2005/06/02	4.01	36.14	−89.46	28
Marston	2006/10/18	3.41	36.54	−89.64	4
Whiting	2010/03/02	3.40	36.79	−89.36	9
Bardwell	2003/06/06	4.05	36.87	−88.98	4
Mineral	2011/08/23	5.74	37.91	−77.98	5
Mineral	2011/08/25	3.97	37.94	−77.90	3
Caborn	2002/06/18	4.55	37.98	−87.80	5
Sullivan	2011/06/07	3.89	38.12	−90.93	110
MtCarmel	2008/04/18	5.30	38.45	−87.89	29
MtCarmel	2008/04/25	3.75	38.45	−87.87	14
MtCarmel	2008/04/21	4.03	38.47	−87.82	24
MtCarmel	2008/04/18*	4.64	38.48	−87.89	23
Greentown	2010/12/30	3.85	40.43	−85.89	8
PrairieCntr	2004/06/28	4.18	41.44	−88.94	8

*Aftershock.

Source Term

To investigate the effect of magnitude on the V/H response spectral ratio, we categorized the database into three distance ranges ($R_{\mathrm{Rup}} \le 100$ km, 100 km $\le R_{\mathrm{Rup}} \le 300$ km, and 300 km $\le R_{\mathrm{Rup}} \le 600$ km). The considered distance ranges were chosen to be representative of short, intermediate, and long source-to-site distances based on the availability of records in our database. For each distance category, the data are clustered into 0.1 magnitude bins, and the median V/H response spectral ratio and its associated standard deviation is computed for each cluster. Figure 3 shows how the median V/H spectral ratios for PGA, and 0.1, 1.0, and 2.0 s spectral accelerations scale with magnitude for soil sites ($V_{S30} = 270$ m/s). It should be mentioned that some of the considered magnitude bins are empty in Figure 3, due to the scarcity in data. For short periods ($T \le 0.1$ s), the V/H response spectral ratios for all three distance clusters decay with increasing magnitude up to $\mathbf{M} \sim 4.0$. Although our database is deficient for earthquakes of $\mathbf{M} > 4.0$ at $R_{\mathrm{Rup}} \le 100$ km, the V/H response spectral ratios are approximately magnitude independent for the other distance ranges.

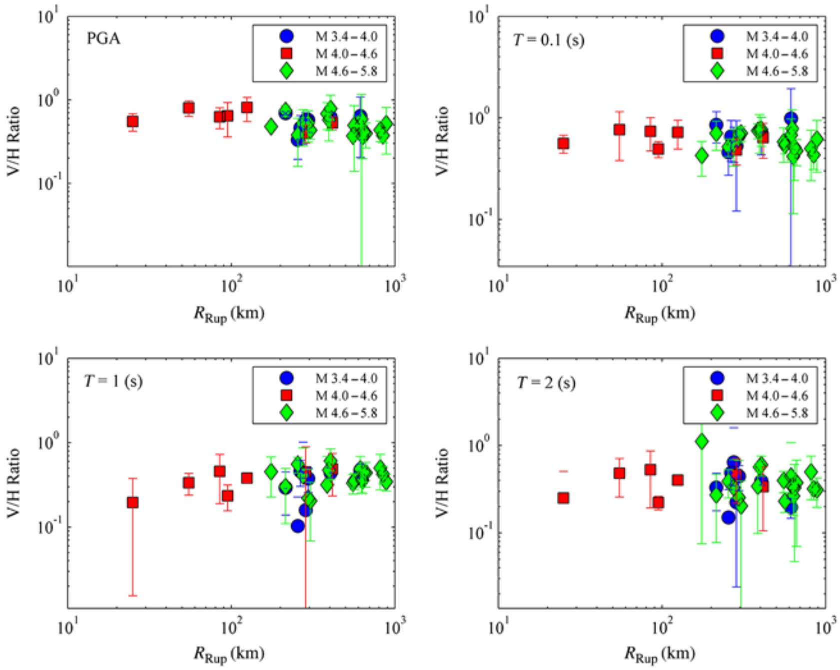

Figure 4. Median V/H response spectral ratios as a function of R_{Rup} for soil sites ($V_{S30} = 270$ m/s). Error bars represent the one standard deviation of each distance bin. The color version of this figure is available only in the electronic edition.

For long periods ($T \geq 1.0$ s), we do not see a significant magnitude dependency in the median V/H response spectral ratios. We tried different functional forms with or without the second-order magnitude term. The statistical p-values from the mixed-effects regression results showed that the second-order magnitude term is statistically insignificant for $\mathbf{M} > 4.0$. Based on examination of various models, the source term was determined to represent the data the best and is expressed as

$$f_{\mathrm{source}} = \begin{cases} a_1 + a_2(\mathbf{M} - \mathbf{M}_h) + a_3(\mathbf{M} - \mathbf{M}_h)^2 & \mathbf{M} \leq \mathbf{M}_h \\ a_1 + a_4(\mathbf{M} - \mathbf{M}_h) & \mathbf{M} > \mathbf{M}_h \end{cases}, \quad (2)$$

in which a_1–a_4 are fixed-effects coefficients, $\mathbf{M}$ is the moment magnitude, and $\mathbf{M}_h$ is the hinge magnitude fixed at 4.0. It is worth mentioning that the style-of-faulting term was initially included in equation (2), yet p-values of the corresponding coefficients revealed that they are statistically insignificant. Furthermore, excluding the style of faulting from equation (2) reduced the total variability by ~10%. Therefore, the style of faulting was not included in the final proposed source term.

Path Term

In general, the path effect is modeled through the effects of anelastic attenuation and geometrical spreading (Zandieh and Pezeshk, 2010; Hosseini *et al.*, 2015; Sedaghati and Pezeshk, 2016, 2017). To investigate the effect of distance on the V/H response spectral ratios, we categorized the database into three magnitude ranges ($3.4 \leq \mathbf{M} < 4.0$, $4.0 \leq \mathbf{M} < 4.6$, and $4.6 \leq \mathbf{M} < 5.8$). For each magnitude range, the data are clustered into 10 km distance bins, and the median V/H response spectral ratio and its associated standard deviation is computed for each cluster. It should be noted that 10 km was the smallest bin in which we would have at least three records to be statistically robust. Figure 4 shows how the median V/H response spectral ratios scale with R_{Rup} for soil sites ($V_{S30} = 270$ m/s) for the considered magnitude ranges. Similar to results reported by Atkinson (1993), the V/H spectral ratio model for the study region has low magnitude dependency. However, as it can be seen from Figure 4, the median V/H response spectral ratios tend to decay with increasing distances for PGA, whereas they are almost distance independent for $T = 0.1$ s. The median V/H spectral ratios start to increase smoothly with distance for $T \geq 1.0$ s. Consequently, the path term is expressed as

$$f_{\mathrm{path}} = a_5 \mathbf{M} \ln\sqrt{(R_{\mathrm{Rup}}^2 + h^2)}, \quad (3)$$

in which a_5 is a fixed-effects coefficient, h is the hypothetical depth coefficient, assumed to be 6.0 km following Pezeshk *et al.* (2015).

Site Term

We did not account for the soil nonlinearity because the magnitude range of the considered database is limited to $3.4 \leq \mathbf{M} < 5.8$. The site term is expressed as

$$f_{\mathrm{site}} = a_6 \ln(V_{S30}/V_{\mathrm{ref}}), \quad (4)$$

in which a_6 is a fixed-effects coefficient, and V_{ref} is equal to 760 m/s. The considered site term is also similar to the employed site term in the PEER NGA-East median GMMs by Hollenback *et al.* (2015) in PEER (2015a).

Variability

Following the notation used by Al Atik *et al.* (2010), the total variability of the ground motion (Δ_{es}) can be separated into the between-events variability (ΔB_e) and the within-event variability (ΔW_{es}), in which the s and e stand for an observation for earthquake e recorded at station s, respectively. The terms ΔB_e and ΔW_{es} have standard deviations τ and φ, respectively. The within-event residual can be decomposed into the site-to-site residual ($\delta S2S$) and the site- and event-corrected residual (δWS_{es}). The standard deviations of the δWS_{es} and $\delta S2S$ are represented by φ_{SS} and φ_{S2S}. The ergodic sigma of the GMMs is typically defined as

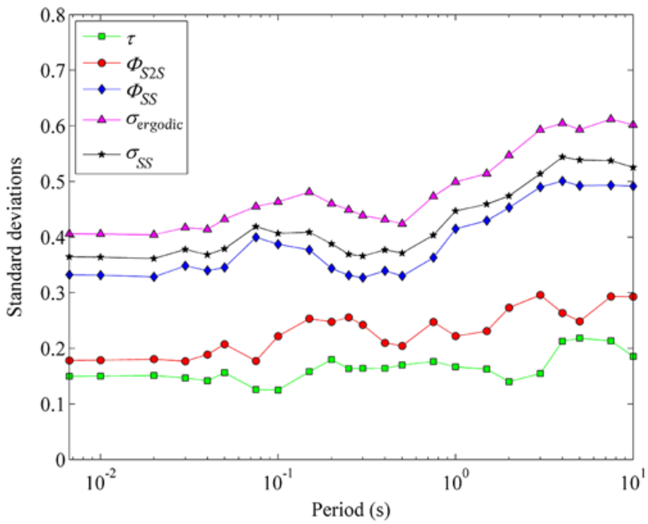

Figure 5. Variations of standard deviations of the proposed V/H model as a function of period. The color version of this figure is available only in the electronic edition.

$$\sigma_{\text{ergodic}} = \sqrt{\tau^2 + \varphi^2}. \quad (5)$$

Equation (5) can be rewritten as

$$\sigma_{\text{ergodic}} = \sqrt{\tau^2 + \varphi_{SS}^2 + \varphi_{S2S}^2}. \quad (6)$$

In recent years, it has been observed that the variability in multiple recordings from similar earthquakes occurring in specific sites is comparably lower than the ergodic sigma values of GMMs (Rodriguez-Marek *et al.*, 2014). This difference is due to the fact that the ergodic sigma includes the site-to-site variations between sites which have been captured using the same site parameter (e.g., V_{S30}), whereas a single site is free of these variations. Therefore, if the site term ($\delta S2S$) is known, its standard deviation (φ_{S2S}) can be excluded from equation (6), such that

$$\sigma_{ss} = \sqrt{\tau^2 + \varphi_{SS}^2}, \quad (7)$$

in which σ_{ss} is referred to as single-station sigma (Atkinson, 2006). The application of single-station sigma is referred to as a partially nonergodic PSHA approach, in which the aleatory variability and epistemic uncertainties are clearly separated (Rodriguez-Marek *et al.*, 2014).

In this study, a mixed-effect regression is used to obtain the median V/H response spectral ratios for PGA and 5% damped spectral accelerations up to a period of 10.0 s. The corresponding regression coefficients for each spectral period are calculated and tabulated in Table 2. Associated standard deviations of the proposed V/H response spectral ratio model are plotted in Figure 5 as a function of period. Between-events variability has the least contribution to the total standard deviation, as is generally the case for the V/H ratios. This is due to the fact that the correlated between-event terms of horizontal and vertical ground-motion components cancel each other (Bommer *et al.*, 2011). The total ergodic standard deviation varies from about 0.4 at $T = 0.01$ s to about 0.6 at $T = 10.0$ s.

The robustness of the proposed V/H model is investigated by plotting the between-event, site-to-site, and event-site

Table 2
Regression Coefficients of the Proposed Vertical-to-Horizontal (V/H) Response Spectral Ratio Model

Period (s)	a_1	a_2	a_3	a_4	a_5	a_6	τ	φ_{S2S}	φ_{SS}	σ_{ergodic}	σ_{SS}
PGA	−0.5211	−0.1921	0.3878	0.0283	−0.0069	0.0107	0.150	0.178	0.332	0.406	0.365
0.010	−0.5260	−0.1694	0.4286	0.0270	−0.0067	0.0108	0.150	0.179	0.332	0.406	0.364
0.020	−0.4962	−0.1854	0.4282	0.0298	−0.0077	0.0052	0.151	0.181	0.328	0.404	0.362
0.030	−0.4843	−0.2805	0.2962	0.0427	−0.0087	−0.0008	0.147	0.177	0.348	0.417	0.378
0.040	−0.4164	−0.3081	0.3351	0.0570	−0.0114	−0.0145	0.142	0.189	0.340	0.414	0.368
0.050	−0.3135	−0.4459	0.0636	0.0678	−0.0141	−0.0194	0.156	0.207	0.345	0.432	0.379
0.075	−0.3084	−0.5578	−0.2000	0.0468	−0.0117	−0.0199	0.126	0.177	0.400	0.455	0.419
0.100	−0.4506	−0.6176	−0.4195	−0.0039	−0.0037	0.0069	0.125	0.222	0.387	0.463	0.407
0.150	−0.7297	−0.4752	−0.3340	−0.0436	0.0061	0.0226	0.158	0.253	0.377	0.481	0.409
0.200	−0.8907	−0.2079	0.0350	−0.0391	0.0092	0.0281	0.180	0.248	0.344	0.460	0.388
0.250	−0.9477	−0.1886	−0.0947	0.0108	0.0072	0.0194	0.163	0.256	0.331	0.449	0.369
0.300	−0.9234	−0.0614	−0.0488	0.0410	0.0038	0.0166	0.164	0.242	0.327	0.439	0.366
0.400	−0.9581	−0.0039	−0.1275	0.0312	0.0040	0.0116	0.164	0.210	0.339	0.432	0.377
0.500	−1.0488	0.1222	0.1461	−0.0012	0.0078	0.0268	0.170	0.204	0.330	0.424	0.371
0.750	−1.2670	−0.0180	0.1631	−0.0353	0.0165	0.0447	0.176	0.247	0.363	0.473	0.404
1.000	−1.3645	0.1127	0.6148	−0.0285	0.0203	0.1014	0.167	0.222	0.415	0.499	0.447
1.500	−1.3061	0.2303	0.8214	0.0030	0.0173	0.1328	0.163	0.231	0.430	0.514	0.459
2.000	−1.1654	0.1112	0.5613	0.0367	0.0118	0.1609	0.140	0.273	0.453	0.547	0.474
3.000	−1.2135	−0.5044	−0.3204	0.0494	0.0131	0.1571	0.155	0.296	0.490	0.593	0.514
4.000	−1.4130	−1.0095	−0.9466	0.0159	0.0209	0.1589	0.213	0.264	0.501	0.605	0.544
5.000	−1.5017	−0.7197	−0.2040	−0.0430	0.0251	0.1662	0.218	0.249	0.492	0.593	0.539
7.500	−1.4562	−0.2013	0.5260	−0.0743	0.0245	0.1788	0.213	0.293	0.493	0.612	0.537
10.00	−1.3588	0.2686	0.9858	−0.0471	0.0207	0.1893	0.185	0.293	0.492	0.602	0.525

PGA, peak ground acceleration; $\delta S2S$, site-to-site residual; δWS_{es}, the site- and event-corrected residual.

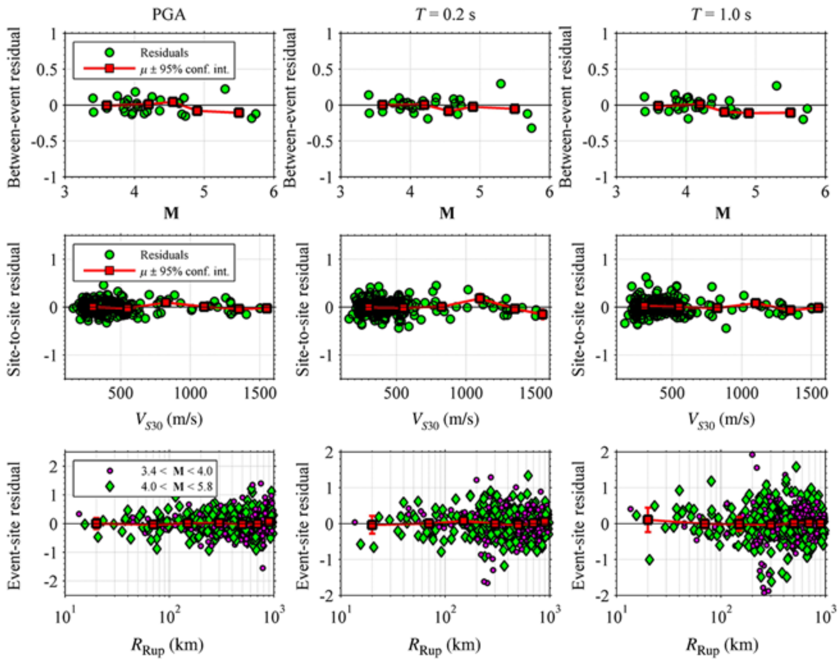

Figure 6. Between-event, site-to-site, and event-site residuals for peak ground acceleration (PGA), $T = 0.2$ s, and $T = 1.0$ s. The color version of this figure is available only in the electronic edition.

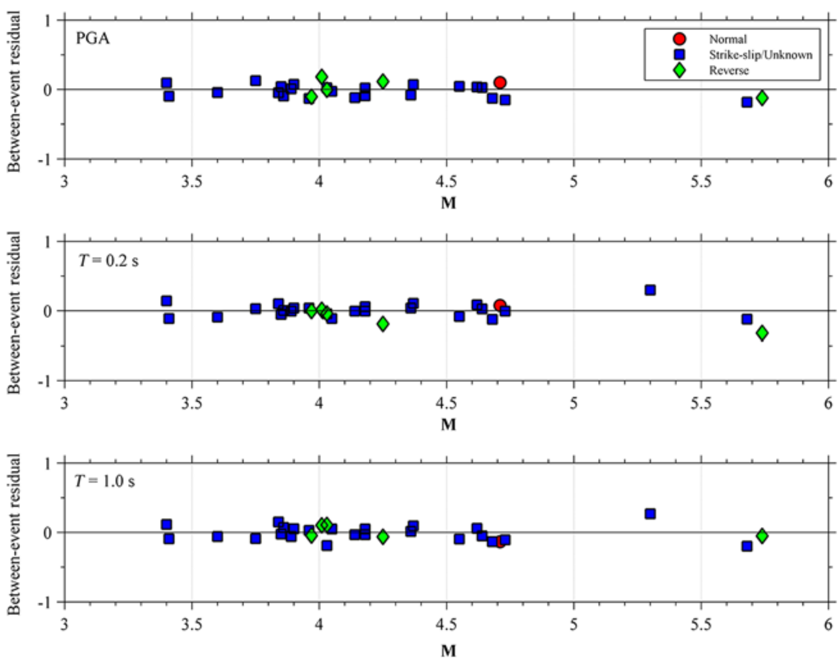

Figure 7. Between-event residuals in terms of style of faulting for PGA, $T = 0.2$ s, and $T = 1.0$ s. The color version of this figure is available only in the electronic edition.

corrected residuals for a range of spectral periods. Figure 6 illustrates the sufficiency of the proposed source term (**M** scaling), site term (V_{S30} scaling), and path term (distance scaling) for PGA, $T = 0.1$ s, and $T = 1.0$ s. A straight line is also fitted to the residuals with its 95% confidence interval for a better trend visualization. Zero mean residuals, which are uncorrelated with respect to the input parameters, would confirm an unbiased model in our regression. As can be observed, the residuals are randomly distributed, and there is no discernible trend in the regression model residuals versus different input parameters. Similar results were obtained at other spectral periods as well. Figure 7 shows the residual analysis to capture the effect of faulting, which was not included in our proposed model. As can be seen from Figure 7, the residuals do not depend on the style of faulting.

Predicted V/H Spectral Ratios

Variations in the predicted median V/H response spectral ratios as a function of distance, magnitude, and V_{S30} are presented in this section. Figure 8 shows the variation of median V/H response spectral ratio as a function of period for a range of rupture distances and magnitudes for soil sites ($V_{S30} = 270$ m/s). As can be observed from Figure 8, the median V/H response spectral ratios increase with increasing magnitudes in the short-period ranges ($T \leq 0.1$ s), with pronounced effects at short rupture distances. A similar magnitude dependency in V/H response spectral ratios is seen for longer periods ($T > 0.2$ s) with pronounced behavior at longer rupture distances. The V/H response spectral ratio peaks at around $T = 0.05$ s and attenuates rapidly with increasing rupture distance.

Figure 9 illustrates the median V/H response spectral ratios as a function of period for a range of small-to-large magnitude earthquakes occurring at a rupture distance of 5 km on different site conditions. As shown in Figure 9, the site term does not influence the median V/H ratios for $T \leq 0.2$. Interestingly, the V/H ratios increase at long periods with increasing V_{S30}. This is due to the stronger V_{S30} dependency of the horizontal component of earthquake ground motions compared to the vertical component (Abrahamson and Silva, 1997).

Comparison with Other Studies

For the first set of comparisons, the proposed model is compared with the predicted V/H response spectral ratios from Gülerce and Abrahamson (2011; hereafter, GA11), Bommer

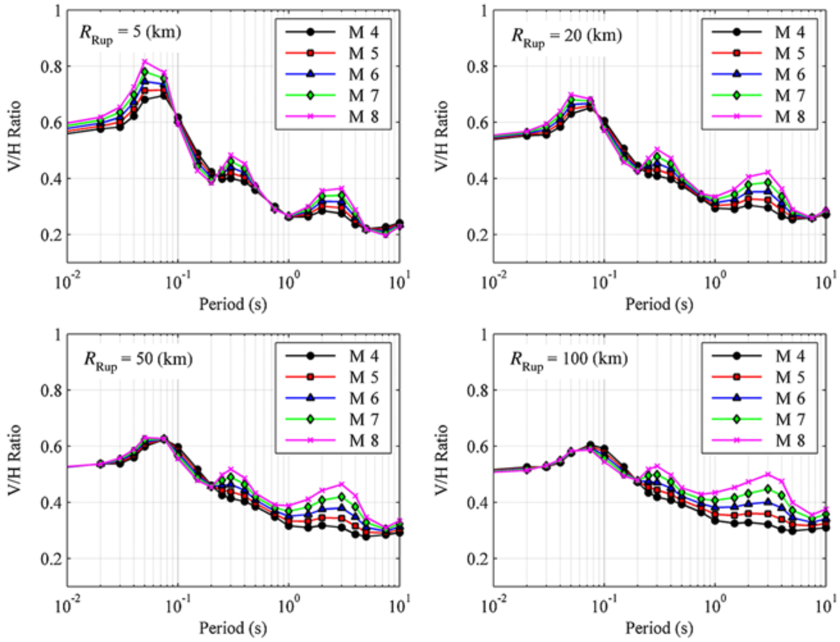

Figure 8. The proposed median V/H response spectral ratios as a function of the period for a range of magnitudes and rupture distances on a soil site condition ($V_{S30} = 270$ m/s). The color version of this figure is available only in the electronic edition.

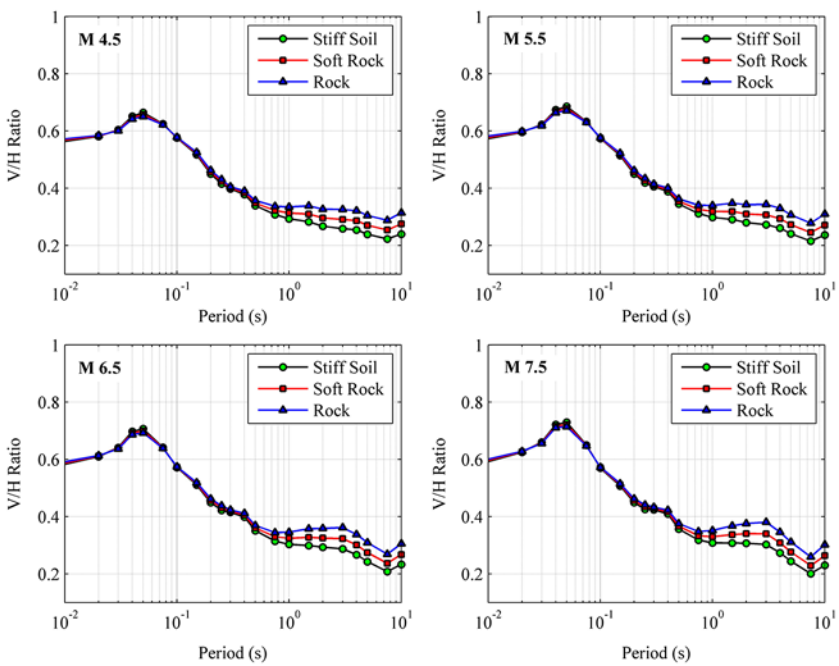

Figure 9. The proposed median V/H response spectral ratios as a function of the period for a range of magnitudes and different soil site conditions at a rupture distance of 5 km. The color version of this figure is available only in the electronic edition.

et al. (2011; hereafter, BAK11), Akkar *et al.* (2014; hereafter, ASA14), and Sedaghati and Pezeshk (2017; hereafter, SP17). The comparison plots are provided in Figure 10 for a scenario earthquake of **M** 5.5 at a rupture distance of 50 km for both soil ($V_{S30} = 270$ m/s) and rock sites ($V_{S30} = 760$ m/s). The models compared herein are all plotted for the spectral period ranges suggested by the model developers. The immediate observation from the comparison plots confirms the general trend of the V/H response spectral ratios which are (1) higher at high frequencies than at low frequencies and (2) lower on rock site than on soil site. As can be seen from Figure 10, the proposed V/H spectral ratios are lower than the V/H response spectral ratios of GA11, especially for soil sites while it is in general agreement with the ASA14 and SP17 models. For rock sites, the predicted V/H ratios approximately flatten out, whereas the other models show an overall increasing trend.

The last set of comparison plots are presented in Figure 11, similar to Figure 10. We calculated the median V/H response spectral ratios using the ratio of the NGA-West2 vertical and horizontal GMPEs developed as part of the NGA-West2 project (Chiou and Youngs, 2013, in PEER 2013, hereafter, CY13; Bozorgnia *et al.*, 2014; Bozorgnia and Campbell, 2016b, hereafter, BC16; Stewart *et al.*, 2016, hereafter, SSBA16; and Gülerce *et al.*, 2017, hereafter, GKAS17). In general, the NGA-West2 V/H ratios follow fairly the same trend for soil sites. However, they differ significantly in longer periods, specifically for rock sites. The proposed model is showing constant and lower V/H ratio values for longer periods when compared with the other empirical models. The observed difference could be due to the high-pass filtering (significantly less than 0.1 Hz) in the NGA-East database with these smaller magnitude events and the larger distances. For soil sites, the proposed model predictions are lower in short-period ranges ($T > 0.1$ s) compared with the NGA-West2 ratios. Similar to Figure 10, the peak point in longer periods for our model is smaller compared with the NGA-West2 models. The difference between various models can be attributed to the tectonic and geological differences of regions for which the models were developed and the database differences, specifically the magnitude ranges.

Summary and Conclusions

A model for the prediction of median V/H response spectral ratios for the Gulf Coast region is presented in this article using a subset of the NGA-East database with magnitudes

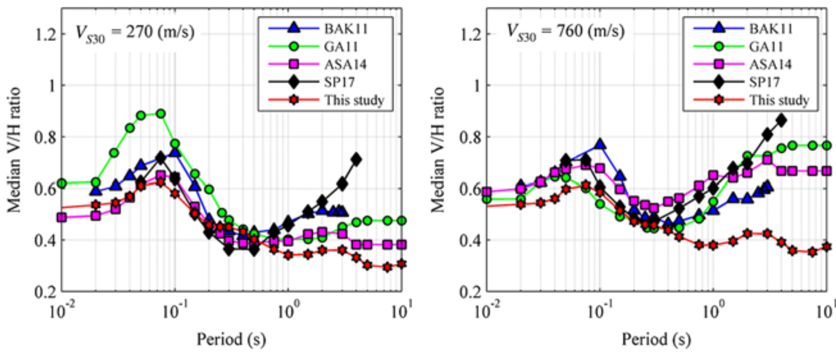

Figure 10. The proposed V/H response spectral ratio model in comparison with the BAK11 (Bommer *et al.*, 2011), GA11 (Gülerce and Abrahamson, 2011), ASA14 (Akkar *et al.*, 2014), and SP17 (Sedaghati and Pezeshk, 2017) models using **M** 5.5 and $R_{\mathrm{Rup}} =$ 50 km for soil ($V_{S30} = 270$ m/s) and rock ($V_{S30} = 760$ m/s) site conditions. The color version of this figure is available only in the electronic edition.

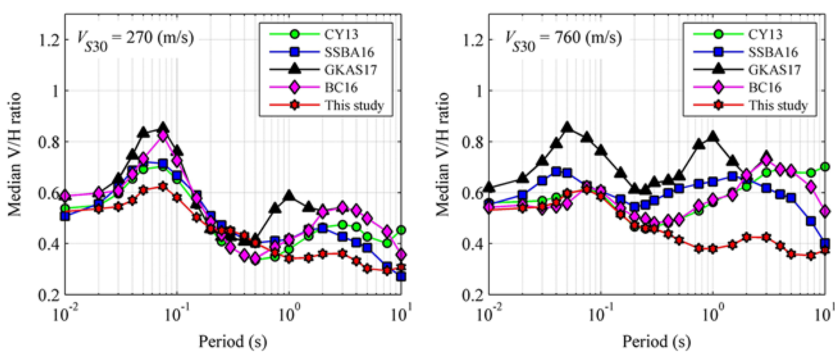

Figure 11. The proposed V/H response spectral ratio model in comparison with the CY13 (Chiou and Youngs, 2013, in PEER 2013), SSBA16 (Stewart *et al.*, 2016), GKAS17 (Gülerce *et al.*, 2017), and BC16 (Bozorgnia and Campbell, 2016b) models using **M** 5.5 and $R_{\mathrm{Rup}} = 50$ km for soil ($V_{S30} = 270$ m/s) and rock ($V_{S30} = 760$ m/s) site conditions. The color version of this figure is available only in the electronic edition.

ranging from **M** 3.4 to 5.74 and rupture distances ranging from 20 to 1000 km. The presented model has the advantage of considering magnitude, source-to-site distance, and shear-wave velocity of soil deposits in the upper 30 m of the site in a wide period range of up to 10.0 s. It should be mentioned that we considered long source-to-site distances to be sufficient, based on the deaggregation analysis of PSHA in the Gulf Coast region. Having said that, the review of past earthquakes shows that the region is capable of producing events with magnitudes greater than 5.74 in the future. Scarcity data are noticeable in developing empirical relations, such as GMPEs and V/H ratio models for the region. We are aware that the magnitude range of events used in this study is a limitation for the developed model, but we also believe that the developed model provides a foundation for calculating V/H ratios and vertical spectrum based on the available data. For applications outside the input magnitude and distance, the model should be used with caution. The presented model is the first V/H model derived specifically for application in the Gulf Coast region to address a lack of suitable models in this region. The proposed model is compared with recent V/H models and the ratio of the V/H NGA-West2 GMPEs. We plan to expand this study to cover the whole CENA in future articles.

Data and Resources

The seismograms used in this study are from the Next Generation Attenuation (NGA)-East database available at http://ngawest2.berkeley.edu/ (last accessed June 2016). The regression analysis was performed using MATLAB mixed-effects regression functions of *nlmefit* and *fitlmematrix* (MathWorks Inc., 2015).

Acknowledgments

The authors wish to thank Yousef Bozorgnia for providing the database of the ground motions for the Gulf Coast region. The authors also like to thank Julian J. Bommer, Zeynep Gülerce, Nick Gregor, and two anonymous reviewers for providing constructive recommendations.

References

Abrahamson, N. A., and W. Silva (1997). Empirical response spectral attenuation relations for shallow crustal earthquakes, *Seismol. Res. Lett.* **68,** 94–127.

Abrahamson, N. A., and W. J. Silva (2008). Summary of the Abrahamson & Silva NGA ground-motion relations, *Earthq. Spectra* **24,** 67–97.

Akkar, S., and J. J. Bommer (2006). Influence of long-period filter cut-off on elastic spectral displacements, *Earthq. Eng. Struct. Dynam.* **35,** 1145–1165.

Akkar, S., Ö. Kale, E. Yenier, and J. J. Bommer (2011). The high-frequency limit of usable response spectral ordinates from filtered analogue and digital strong-motion accelerograms, *Earthq. Eng. Struct. Dynam.* **40,** doi: 10.1002/eqe.1095.

Akkar, S., M. A. Sandıkkaya, and B. Ö. Ay (2014). Compatible ground motion prediction equations for damping scaling factors and vertical-to-horizontal spectral amplitude ratios for the broader Europe region, *Bull. Earthq. Eng.* **12,** 517–547.

Akkar, S., M. A. Sandıkkaya, and J. J. Bommer (2013a). Empirical ground-motion models for point- and extended-source crustal earthquake scenarios in Europe and the Middle East, *Bull. Earthq. Eng.* **12,** doi: 10.1007/s10518-013-9461-4.

Akkar, S., M. A. Sandıkkaya, and J. J. Bommer (2013b). Erratum to "Empirical ground-motion models for point- and extended-source crustal earthquake scenarios in Europe and the Middle East," *Bull. Earthq. Eng.* **12,** doi: 10.1007/s10518-013-9508-6.

Al Atik, L., N. A. Abrahamson, J. J. Bommer, F. Scherbaum, F. Cotton, and N. Kuehn (2010). The variability of ground motion prediction models and its components, *Seismol. Res. Lett.* **81,** 794–801.

Ambraseys, N. N., and J. Douglas (2003). Near-field horizontal and vertical earthquake ground motions, *Soil Dynam. Earthq. Eng.* **23,** 1–18.

Atkinson, G. M. (1993). Notes on ground motion parameters for eastern North America: Duration and H/V ratio, *Bull. Seismol. Soc. Am.* **83,** 587–596.

Atkinson, G. M. (2006). Single-station sigma, *Bull. Seismol. Soc. Am.* **96,** 446–455.

Bommer, J. J., S. Akkar, and Ö. Kale (2011). A model for vertical-to-horizontal response spectral ratios for Europe and the Middle East, *Bull. Seismol. Soc. Am.* **101,** 1783–1806.

Boore, D. M. (2010). Orientation-independent, nongeometric-mean measures of seismic intensity from two horizontal components of motion, *Bull. Seismol. Soc. Am.* **100,** 1830–1835.

Boore, D. M., and J. J. Bommer (2005). Processing of strong motion accelerograms: Needs, options and consequences, *Soil. Dynam. Earthq. Eng.* **25,** 93–115.

Boore, D. M., and C. A. Goulet (2014). The effect of sampling rate and anti-aliasing filters on high-frequency response spectra, *Bull. Earthq. Eng.* **12,** 203–216.

Bozorgnia, Y., and K. W. Campbell (2004a). Engineering characterization of ground motion, in *Earthquake Engineering: From Engineering Seismology to Performance-Based Engineering*, Y. Bozorgnia and V. V. Bertero (Editors), CRC Press, Boca Raton, Florida, 215–315.

Bozorgnia, Y., and K. W. Campbell (2004b). The vertical-to-horizontal response spectral ratio and tentative procedures for developing simplified V/H and vertical design spectra, *J. Earthq. Eng.* **8,** no. 2, 539–561.

Bozorgnia, Y., and K. W. Campbell (2016a). Vertical ground motion model for PGA, PGV, and linear response spectra using the NGA-West2 database, *Earthq. Spectra* **32,** 979–1004.

Bozorgnia, Y., and K. W. Campbell (2016b). Ground motion model for the vertical-to-horizontal (V/H) ratios of PGA, PGV, and response spectra, *Earthq. Spectra* **32,** 951–978.

Bozorgnia, Y., N. A. Abrahamson, L. Al Atik, T. D. Ancheta, G. M. Atkinson, J. W. Baker, A. Baltay, D. M. Boore, K. W. Campbell, B. S.-J Chiou, *et al.* (2014). NGAWest2 research project, *Earthq. Spectra* **30,** 973–987.

Burnham, K. P., and D. R. Anderson (2002). *Model Selection and Multimodel Inference: A Practical Information-Theoretic Approach*, Second Ed., Springer-Verlag, New York, New York, ISBN: 0-387-95364-7.

Campbell, K. W., and Y. Bozorgnia (2014). NGA-West2 ground motion model for the average horizontal components of PGA, PGV, and 5%-damped linear acceleration response spectra, *Earthq. Spectra* **30,** 1087–1115.

Douglas, J., and D. M. Boore (2011). High-frequency filtering of strong motion records, *Bull. Earthq. Eng.* **9,** 395–409.

Dreiling, J., M. P. Isken, W. D. Mooney, M. C. Chapman, and R. W. Godbee (2014). NGA-East regionalization report: Comparison of four crustal regions within Central and Eastern North America using waveform modeling and 5%-damped pseudo-spectral acceleration response, *PEER Report 2014/15*, Pacific Earthquake Engineering Research Center (PEER), University of California, Berkeley, California.

Eurocode 8 (2004). Design of structures for earthquake resistance, Part 1: General rules, seismic actions, and rules for buildings, EN 1998-1, European Committee for Standardization (CEN), Brussels, Belgium.

Goulet, C. A., T. Kishida, T. D. Ancheta, C. H. Cramer, R. B. Darragh, W. J. Silva, Y. M. A. Hashash, J. Harmon, J. P. Stewart, K. E. Wooddell, *et al.* (2014). PEER NGA-East database, *PEER Report 2014/17*, Pacific Earthquake Engineering Research Center (PEER), University of California, Berkeley, California.

Graizer, V. (2012). Effect of low-pass filtering and re-sampling on spectral and peak ground acceleration in strong-motion records, *Proc. of the 15th World Conference of Earthquake Engineering*, Lisbon, Portugal, 24–28 September 2012, 10 pp.

Gülerce, Z., and N. A. Abrahamson (2011). Site-specific design spectra for vertical ground motion, *Earthq. Spectra* **27,** 1023–1047.

Gülerce, Z., R. Kamai, N. A. Abrahamson, and W. J. Silva (2017). Ground motion prediction equations for the vertical ground motion component based on the NGA-W2 database, *Earthq. Spectra* **33,** no. 2, 499–528.

Hosseini, M., S. Pezeshk, A. Haji-Soltani, and M. Chapman (2015). Investigation of attenuation of the *Lg*-wave amplitude in the Caribbean region, *Bull. Seismol. Soc. Am.* **105,** 734–744.

Kunnath, S. K., E. Erduran, Y. H. Chai, and M. Yashinsky (2008). Effect of near-fault vertical ground motions on seismic response of highway overcrossings, *J. Bridge Eng.* **13,** 282–290.

Lindstrom, M. J., and D. M. Bates (1990). Nonlinear mixed effects models for repeated measures data, *Biometrics* **46,** 673–687.

MathWorks Inc. (2015). *MATLAB and Statistics and Machine Learning Toolbox*, Release 2015a, The MathWorks Inc., Natick, Massachusetts.

McGuire, R. K., W. J. Silva, and C. J. Costantino (2001). Technical basis for revision of regulatory guidance on design ground motions: Hazard and risk-consistent ground motion spectra guidelines, *U.S. Nuclear Regulatory Commission NUREG/CR-6728*, Washington, D.C., 1020 pp.

National Earthquake Hazards Reduction Program (NEHRP) (2009). *2009 NEHRP Recommended Seismic Provisions for New Buildings and other Structures. Part 1, Provisions*, National Earthquake Hazards Reduction Program, Washington D.C., 373 pp.

Pacific Earthquake Engineering Research Center (PEER) (2013). NGA-West2 Ground Motion Prediction Equations for Vertical Ground Motions, *PEER Rept. No. 2013/24*, Pacific Earthquake Engineering Research Center, http://peer.berkeley.edu/publications/peer_reports/reports_2013/reports_2013.html (last accessed June 2016).

Pacific Earthquake Engineering Research Center (PEER) (2015a). NGA-East: Median Ground-Motion Models for the Central and Eastern North America Region, *PEER Rept. No. 2015/04*, Pacific Earthquake Engineering Research Center, http://peer.berkeley.edu/publications/peer_reports/reports_2015/reports_2015.html (last accessed June 2016).

Pacific Earthquake Engineering Research Center (PEER) (2015b). NGA-East: Adjustments to Median Ground-Motion Models for Central and Eastern North America, *PEER Rept. No. 2015/08*, Pacific Earthquake Engineering Research Center, http://peer.berkeley.edu/publications/peer_reports/reports_2015/reports_2015.html (last accessed June 2016).

Papazoglou, A. J., and A. S. Elnashai (1996). Analytical and field evidence of the damaging effect of vertical earthquake ground motion, *Earthq. Eng. Struct. Dynam.* **25,** 1109–1138.

Pezeshk, S., A. Zandieh, K. W. Campbell, and B. Tavakoli (2015). Ground-motion prediction equations for CENA using the hybrid empirical method in conjunction with NGA-West2 empirical ground-motion models, Chapter 5, *PEER Report 2015/04*, Pacific Earthquake Engineering Research Center (PEER), University of California, Berkeley, California.

Rodriguez-Marek, A., E. M. Rathje, J. J. Bommer, F. Scherbaum, and P. J. Stafford (2014). Application of single-station sigma and site-response characterization in a probabilistic seismic-hazard analysis for a new nuclear site, *Bull. Seismol. Soc. Am.* **104,** 1601–1619.

Saadeghvaziri, M., and D. A. Foutch (1991). Dynamic behavior of R/C highway bridges under the combined effect of vertical and horizontal earthquake motions, *Earthq. Eng. Struct. Dynam.* **20,** 535–549.

Sedaghati, F., and S. Pezeshk (2016). Estimation of the coda-wave attenuation and geometrical spreading in the New Madrid seismic zone, *Bull. Seismol. Soc. Am.* **106,** 1482–1498.

Sedaghati, F., and S. Pezeshk (2017). Partially nonergodic empirical ground motion models for predicting horizontal and vertical PGV, PGA, and 5% damped linear acceleration response spectra using data from Iranian plateau, *Bull. Seismol. Soc. Am.* **107,** 934–948.

Siddiqqi, J., and G. Atkinson (2002). Ground-motion amplification at rock sites across Canada as determined from the horizontal-to-vertical component ratio, *Bull. Seismol. Soc. Am.* **92,** 877–884.

Stewart, J. P., D. M. Boore, E. Seyhan, and G. M. Atkinson (2016). NGA-West2 equations for predicting vertical-component PGA, PGV, and 5%-damped PSA from shallow crustal earthquakes, *Earthq. Spectra* **32,** 1005–1031.

Walling, M., W. Silva, and N. A. Abrahamson (2008). Nonlinear site amplification factors for constraining the NGA models, *Earthq. Spectra* **24,** 243–255.

Yu, C. P., D. S. Broekhuizen, and J. M. Roesset (1997). Effect of vertical ground motion on bridge deck response, *Proc. Workshop on Earthquake Engineering Frontiers in Transportation Facilities, Tech. Rept. NCEER 97-0005*, U.S. National Center for Earthquake Engineering Research (NCEER); Japan International Center for Disaster Mitigation Engineering (INCEDE), 249–263.

Zandieh, A., and S. Pezeshk (2010). Investigation of geometrical spreading and quality factor functions in the New Madrid seismic zone, *Bull. Seismol. Soc. Am.* **100,** 2010–2185.

Zandieh, A., and S. Pezeshk (2011). A study of horizontal-to-vertical component spectral ratio in the New Madrid seismic zone, *Bull. Seismol. Soc. Am.* **101,** 287–296.

Mueser Rutledge Consulting Engineers
14 Penn Plaza, 225 W 34th Street
New York, New York 10122
ahaji-soltani@mrce.com
(A.H.-S.)

Department of Civil Engineering
The University of Memphis
Engineering Science Building, Room 104A
Memphis, Tennessee 38152
spezeshk@memphis.edu
(S.P.)

WSP-USA
1 Pennsylvania Plaza
New York, New York 10119
malekm@pbworld.com
(M.M.)

Lettis Consultants International
4155 Darley Avenue
Boulder, Colorado 80305
arash.zandieh@live.com
(A.Z.)

Manuscript received 3 August 2016;
Published Online 25 September 2017